GEOGRAPHICAL REPORTS
OF TOKYO METROPOLITAN UNIVERSITY 57 (2022) 55–62

# DETECTION OF FUJI HOEI TEPHRA PRODUCED BY MT. FUJI VOLCANO IN 1707 (HOEI) PRESENT IN THE MD01-2421 SEDIMENT CORE COLLECTED OFF THE KASHIMA COAST OF EAST JAPAN

**Kaori AOKI**

*Abstract* For cryptotephra detection, data from 419 volcanic glass shards in the deposits from the top of the core to a depth of 9.5 cm from the MD01-2421 core collected off the Kashima coast, East Japan were obtained and divided into seven clusters. The basaltic cluster, andesitic cluster and some volcanic glass shards in the dacitic cluster might be correlated to the Fuji Hoei (F-Ho) tephra that erupted from Mt. Fuji in 1707 AD. A dacitic cluster might include volcanic glass shards originating from another dacitic source magma in addition to Asama A (As-A) tephra erupting from Mt. Asama in 1783 AD and F-Ho tephra.

**Keywords:** marine sediment, Fuji Hoei eruption, 1707 AD, Asama A tephra

## 1. Introduction

Research on deep-sea sediment samples not only reconstructs the paleoenvironment from multiple perspectives by using various proxies based on physicochemical analysis but can also detect the zone of very fine concentrated volcanic glass shards that can serve as an excellent time marker. Aoki (2021) reported a method for handling residues from foraminiferal research samples from the MD01-2421 core collected off the Kashima coast, East Japan, which was used for cryptotephra detection (Fig. 1). In Aoki (2021), based on the possible correlative tephra in the top 0–9.50 cm of the sediment from the MD01-2412 core and utilizing $^{14}C$ dating for the samples, four eruptive events were identified: the Sakurajima Taisho eruption in 1914 AD (Sz-Ts tephra), Asama Tenmei eruption (As-A tephra) in 1783 AD, the Tarumae eruption (Ta-a tephra) in 1739, and Fuji Hoei eruption (F-Ho tephra) in 1707 AD. Then, it was shown that volcanic glass shards in the cluster with sample properties ranging from rhyolite to dacite could be correlated to the As-A tephra that erupted from Mt. Asama in 1783 AD, compared with the dataset of tephra erupted from Mt. Asama described in Aoki (2020).

This report discusses the comparison and correlations between the above dataset of MD01-2412 in Aoki (2021) and the geochemistry of the F-Ho tephra from Mt Fuji in 1707 AD (Watanabe *et al*. 2006).

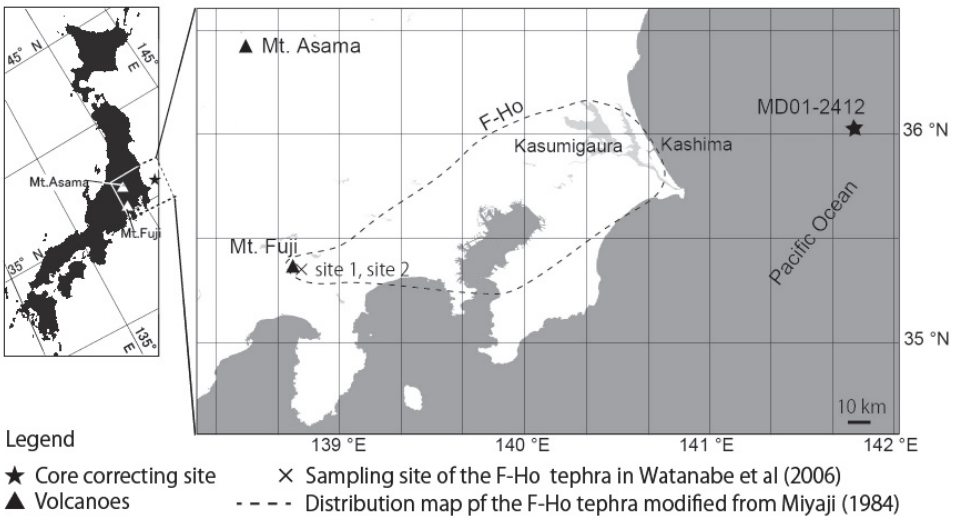


**Fig. 1** Location map of sediment core and volcanoes.
Site 1 and site 2 (×) are sampling sites of F-Ho tephra in Watanabe *et al*. (2006).

## 2. Summary of research samples and dataset of volcanic glass shards

### Summary of research samples and dataset

Core MD01-2421, which was used in this study, was collected approximately 100 km east of the Kashima coast by a giant piston corer on the French marine research vessel "Marion Dufresne" during the 7th voyage of the IMAGES Western Pacific Ocean in 2001 (36° 01.4' North latitude, 141° 46.8' East longitude; water depth 2,224 m; Fig. 1). The core length was 45.82 m as measured onboard. The core diameter was 10 cm and the core was mainly composed of olive-gray silty clay, which was interbedded with thin sand layers in places (Oba *et al.* 2006). Oba *et al*. (2006) reported that this core showed continuous deposition since Marine Isotope Stage (MIS) 6.3 based on the oxygen isotope stratigraphy of its planktonic foraminifera and its $^{14}C$ age. In addition, seven layers of widespread tephra among 23 tephra layers interbedded in core MD01-2421 were identified (Aoki 2008; Aoki *et al*. 2008).

To detect cryptotephra at the top of core MD01-2421, Aoki (2021) reused the residues of samples from foraminiferal research samples. The residues were carefully divided to maintain the foraminiferal community composition in the samples. Furthermore, when the sample was sealed with epoxy resin and polished, because there was a large difference in the specific gravity between basaltic particles and rhyolite particles, classification using magnets was performed with samples fixed in resin. As a result, data from 419 volcanic glass shards in the deposits from the top of the core to a depth of 9.5 cm were determined by electron probe microanalyzer (EPMA), and cluster analysis using elemental composition was performed after normalizing the datasets. The seven clusters in Aoki (2021) were classified as follows: Cluster No. 1 and Cluster No. 2 were classified as rhyolite; Cluster No. 3 was classified as andesite; Cluster No. 4 was classified as rhyolite to dacite; and Cluster No. 5, Cluster No. 6, and Cluster No. 7 were classified as basaltic andesite (Fig. 2).

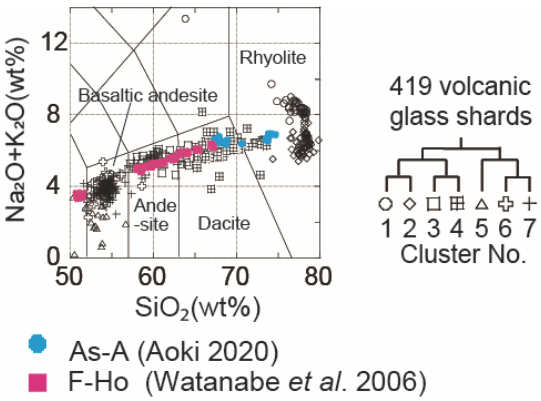


**Fig. 2** Plots of $SiO_2$-$Na_2O$+$K_2O$ of 419 volcanic glass shards from the samples (0-9.5 cm; Aoki 2021), Asama A tephra (As-A; Aoki 2020) and Fuji Hoei tephra (F-Ho; Watanabe *et al.* 2006), based on the rock classification of Le Bas and Streckeisen (1991).
Dendrogram was created by the cluster analysis for geochemistry of 419 volcanic glass shards based on the normalized data-set by a total of each data shown as weight % (Shown in Aoki 2021 as Case A)

**Geochemistry of Fuji Hoei tephra (F-Ho) in 1707 AD**

Mt. Fuji is located in south-central Honshu Japan (Fig. 1). The edifice of Mt. Fuji consists of three volcanoes, which were named Komitake, Older Fuji, and Younger Fuji by Tsuya (1955). The most recent eruption in 1707 AD was the most explosive eruption in the volcanic history of Younger Fuji, Mt Fuji (Tsuya 1955). The eruptive history of Mt. Fuji has been dominated by basaltic volcanism; however, the geochemistry of Fuji Hoei eruptive production in 1707 AD ranges from basalt to dacite (Tsuya 1955; Miyaji 1984). The Plinian eruptions producing andesitic and dacitic pumice deposits began on December 16, 1707; afterward, a Plinian basaltic eruption began and lasted until January 1, 1708 (Koyama *et al*. 1998). Miyaji (1984) described each fall unit of eruptive production and divided four units, Ho I, Ho II, Ho III, and Ho IV in ascend order (Fig. 3), based on grain sizes and constituents. Furthermore, Miyaji (1984) presented the distribution map for each unit and calculated the total eruptive volume (Fig. 1).

Watanabe *et al*. (2006) showed the geochemistry of a proximal sample series of Ho I, Ho II, Ho III, and Ho IV collected at site 1 and site 2 near the source crater (Fig. 1; Fig. 3) and discussed the magmatic systems of the 1707 eruption at the point of evolution of a chemically zoned magma chamber of Mt. Fuji. Their geochemical data of scoria and pumice grains were determined by DCP-AES (direct-current plasma atomic emission spectrometry). They utilized the method using heavy liquid (SPT solution; sodium polytungstate solution) adjusted to a density of 2.45 g/cm$^3$ to purify volcanic glass shards for bulk chemical analysis contrived by Katoh *et al*. (1999) as a pretreatment. The dataset of Watanabe *et al*. (2006) expresses the geochemistry of the matrix in scoria and pumice grains without crystals, namely, parts of volcanic glass. It is allowable to employ the dataset as bulk volcanic glass data by Watanabe *et al*. (2006) (Table 1) for comparison with datasets of volcanic glass shards determined by EPMA (Aoki 2020; 2021).

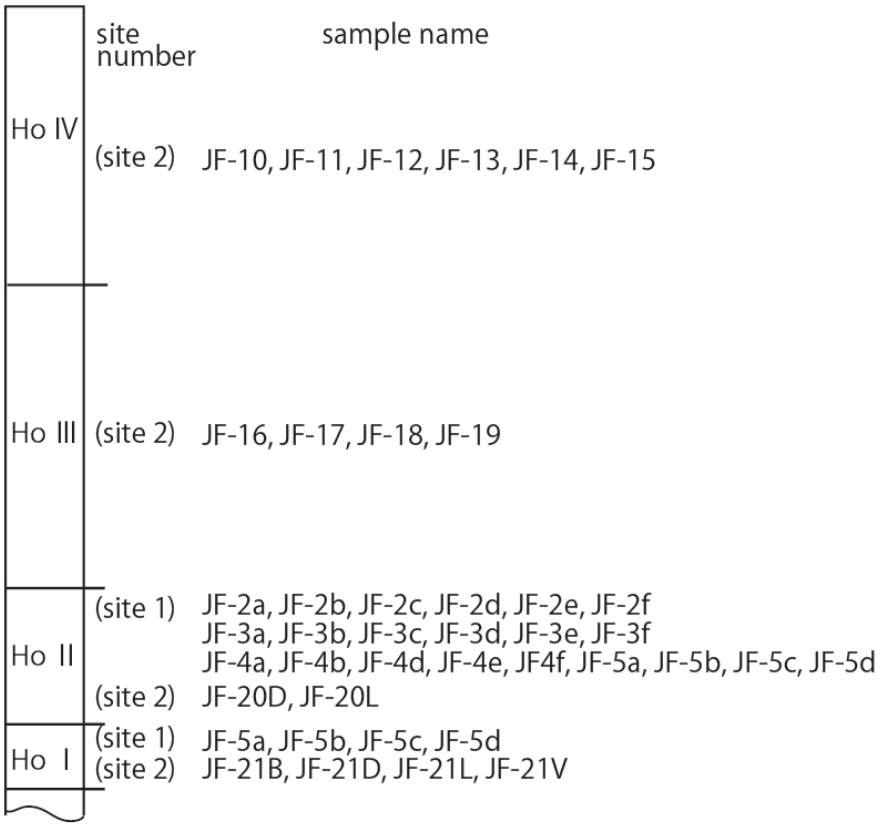


**Fig. 3** Typical stratigraphy of Fuji Hoei tephra and research samples in Watanabe *et al*. (2006). Division of eruptive units is from Miyaji (1984). Site numbers and JF numbers which are sample code name, are shown in Table 1 quoted from Watanabe *et al*. (2006).

## 3. Results and Discussion

On the basis of seven clusters in Case A using the normalized dataset with the total of each data point shown as weight % (Aoki, 2021), the plots of $SiO_2$–$Na_2O$+$K_2O$, $SiO_2$–$Al_2O_3$, $SiO_2$–MgO, $SiO_2$–$Na_2O$, $FeO^{\dagger}$–CaO, and $TiO_2$-$K_2O$ for data from 419 volcanic glass shards in the deposits from the top of the core to a depth of 9.5 cm are shown in Figs. 2 and 4. In addition, the dataset of F-Ho in Table 1 by Watanabe *et al*. (2006) and the data of the volcanic glass shards in the As-A tephra from the Asama Tenmei eruption in 1783 AD, as shown by Aoki (2020), are plotted in Figs. 2 and 4.

**Table 1** Extract of geochemical data of the Fuji Hoei tephra from Table 1 in Watanabe *et al*. (2006) determined major and trace elements by DCP-AES.
Data was recalculated to 100 wt% on a volatile-free basis and Figs.2 and 4 employed these data.

| Site | Sample | units | (wt%) | | | | | | | | | |
|---|---|---|---|---|---|---|---|---|---|---|---|---|
| | | | $SiO_2$ | $TiO_2$ | $Al_2O_3$ | $Fe_2O_3$ | MnO | MgO | CaO | $Na_2O$ | $K_2O$ | $P_2O_5$ |
| Site 1 | JF-2a | Ho II | 57.90 | 1.13 | 16.73 | 8.84 | 0.17 | 3.16 | 6.76 | 3.60 | 1.38 | 0.33 |
| Site 1 | JF-2b | Ho II | 58.57 | 1.09 | 16.67 | 8.52 | 0.16 | 3.01 | 6.55 | 3.63 | 1.43 | 0.36 |
| Site 1 | JF-2c | Ho II | 58.02 | 1.12 | 16.85 | 8.68 | 0.17 | 3.08 | 6.69 | 3.64 | 1.38 | 0.36 |
| Site 1 | JF-2d | Ho II | 60.99 | 0.98 | 16.24 | 7.56 | 0.15 | 2.53 | 5.91 | 3.71 | 1.63 | 0.30 |
| Site 1 | JF-2e | Ho II | 58.70 | 1.09 | 16.75 | 8.48 | 0.16 | 3.00 | 6.47 | 3.62 | 1.43 | 0.31 |
| Site 1 | JF-2f | Ho II | 63.97 | 0.83 | 15.90 | 6.11 | 0.13 | 1.89 | 5.06 | 3.77 | 2.10 | 0.25 |
| Site 1 | JF-3a | Ho II | 62.26 | 0.92 | 16.07 | 7.02 | 0.14 | 2.28 | 5.49 | 3.70 | 1.82 | 0.29 |
| Site 1 | JF-3b | Ho II | 60.37 | 1.01 | 16.27 | 7.88 | 0.15 | 2.66 | 6.09 | 3.62 | 1.64 | 0.31 |
| Site 1 | JF-3c | Ho II | 62.54 | 0.91 | 16.18 | 6.77 | 0.13 | 2.21 | 5.38 | 3.71 | 1.89 | 0.28 |
| Site 1 | JF-3d | Ho II | 59.83 | 1.03 | 16.37 | 8.04 | 0.16 | 2.73 | 6.31 | 3.66 | 1.59 | 0.29 |
| Site 1 | JF-3e | Ho II | 60.63 | 1.00 | 16.41 | 7.68 | 0.15 | 2.57 | 5.96 | 3.69 | 1.61 | 0.29 |
| Site 1 | JF-3f | Ho II | 63.70 | 0.82 | 15.84 | 6.25 | 0.13 | 1.98 | 5.12 | 3.76 | 2.15 | 0.25 |
| Site 1 | JF-4a | Ho II | 59.42 | 1.03 | 16.39 | 8.19 | 0.16 | 2.87 | 6.45 | 3.66 | 1.51 | 0.32 |
| Site 1 | JF-4b | Ho II | 60.19 | 1.02 | 16.56 | 7.81 | 0.15 | 2.64 | 6.04 | 3.67 | 1.58 | 0.32 |
| Site 1 | JF-4d | Ho II | 61.05 | 0.99 | 16.29 | 7.51 | 0.14 | 2.50 | 5.86 | 3.69 | 1.65 | 0.32 |
| Site 1 | JF-4e | Ho II | 64.98 | 0.78 | 15.56 | 5.73 | 0.12 | 1.77 | 4.79 | 3.77 | 2.29 | 0.21 |
| Site 1 | JF-4f | Ho II | 63.29 | 0.84 | 15.91 | 6.41 | 0.13 | 2.00 | 5.24 | 3.84 | 2.08 | 0.27 |
| Site 1 | JF-5a | Ho I | 62.85 | 0.88 | 15.80 | 6.68 | 0.14 | 2.11 | 5.51 | 3.80 | 1.94 | 0.28 |
| Site 1 | JF-5b | Ho I | 62.44 | 0.93 | 16.18 | 6.88 | 0.13 | 2.18 | 5.46 | 3.73 | 1.80 | 0.28 |
| Site 1 | JF-5c | Ho I | 66.82 | 0.68 | 15.21 | 4.89 | 0.11 | 1.44 | 4.28 | 3.83 | 2.53 | 0.21 |
| Site 1 | JF-5d | Ho I | 67.09 | 0.69 | 15.34 | 4.86 | 0.10 | 1.42 | 4.15 | 3.73 | 2.42 | 0.19 |
| Site 2 | JF-10 | Ho IV | 50.69 | 1.36 | 17.16 | 11.99 | 0.19 | 5.29 | 9.64 | 2.72 | 0.73 | 0.23 |
| Site 2 | JF-11 | Ho IV | 51.19 | 1.35 | 17.03 | 11.81 | 0.19 | 5.21 | 9.56 | 2.67 | 0.74 | 0.26 |
| Site 2 | JF-12 | Ho IV | 50.86 | 1.36 | 16.92 | 12.06 | 0.19 | 5.34 | 9.66 | 2.65 | 0.74 | 0.23 |
| Site 2 | JF-13 | Ho IV | 51.03 | 1.35 | 16.84 | 12.02 | 0.19 | 5.31 | 9.56 | 2.63 | 0.72 | 0.35 |
| Site 2 | JF-14 | Ho IV | 50.71 | 1.33 | 17.17 | 11.92 | 0.19 | 5.31 | 9.53 | 2.66 | 0.93 | 0.25 |
| Site 2 | JF-15 | Ho IV | 51.33 | 1.33 | 17.01 | 11.78 | 0.19 | 5.23 | 9.44 | 2.81 | 0.67 | 0.22 |
| Site 2 | JF-16 | Ho IV | 51.04 | 1.33 | 16.92 | 11.93 | 0.19 | 5.37 | 9.64 | 2.61 | 0.72 | 0.25 |
| Site 2 | JF-17 | Ho III | 50.85 | 1.34 | 17.09 | 11.87 | 0.19 | 5.35 | 9.73 | 2.64 | 0.72 | 0.23 |
| Site 2 | JF-18 | Ho III | 51.04 | 1.33 | 16.99 | 11.80 | 0.19 | 5.28 | 9.70 | 2.68 | 0.73 | 0.25 |
| Site 2 | JF-19 | Ho III | 51.38 | 1.33 | 17.11 | 11.56 | 0.19 | 5.11 | 9.51 | 2.78 | 0.80 | 0.24 |
| Site 2 | JF-20L | Ho II | 60.31 | 1.03 | 16.44 | 7.78 | 0.15 | 2.63 | 6.09 | 3.66 | 1.61 | 0.30 |
| Site 2 | JF-20D | Ho II | 58.39 | 1.12 | 16.60 | 8.71 | 0.17 | 3.09 | 6.76 | 3.55 | 1.30 | 0.32 |
| Site 2 | JF-21V | Ho I | 65.34 | 0.75 | 15.49 | 5.62 | 0.12 | 1.71 | 4.70 | 3.75 | 2.29 | 0.23 |
| Site 2 | JF-21L | Ho I | 62.05 | 0.94 | 16.13 | 6.98 | 0.14 | 2.25 | 5.63 | 3.85 | 1.76 | 0.28 |
| Site 2 | JF-21D | Ho I | 59.61 | 1.04 | 16.45 | 8.13 | 0.16 | 2.83 | 6.43 | 3.61 | 1.44 | 0.30 |
| Site 2 | JF-21B | Ho I | 61.84 | 0.95 | 16.17 | 7.12 | 0.14 | 2.31 | 5.69 | 3.73 | 1.78 | 0.29 |

A series of F-Ho determined by DCP-AES plotted in the area ranging from basalt to dacite (Figs. 2 and 4). Generally, when comparing data determined by different methods, careful attention is needed for the idiosyncrasies of each method and the biases in the chemical data. Basaltic magma would have been crystallized by rapid cooling, and it is not unavoidable that

scoria grains would include microlites. Even though the method using heavy liquid to purify volcanic glass shards was examined carefully, it would be difficult to determine the geochemistry of the matrix area in grains more accurately than through microarea scanning analysis such as EPMA. Therefore, it is important to keep in mind that basaltic production data might be affected by microlites.

The chemical composition of the As-A tephra has bimodal characteristics and includes rhyolitic to dacitic volcanic glass shards (Aoki 2020). This composition overlaps with that of Cluster No. 4, which is classified as the area between rhyolite and dacite. On the other hand, many glass shards in the lower $SiO_2$ area in Cluster No. 4 resemble those of F-Ho rather than As-A (Figs. 2 and 4). Geochemistry of volcanic gkass shards ploted in the area of Cluster No. 3 in andesite (Fig. 2) resembles a series of the F-Ho tephra plotted in andesite.

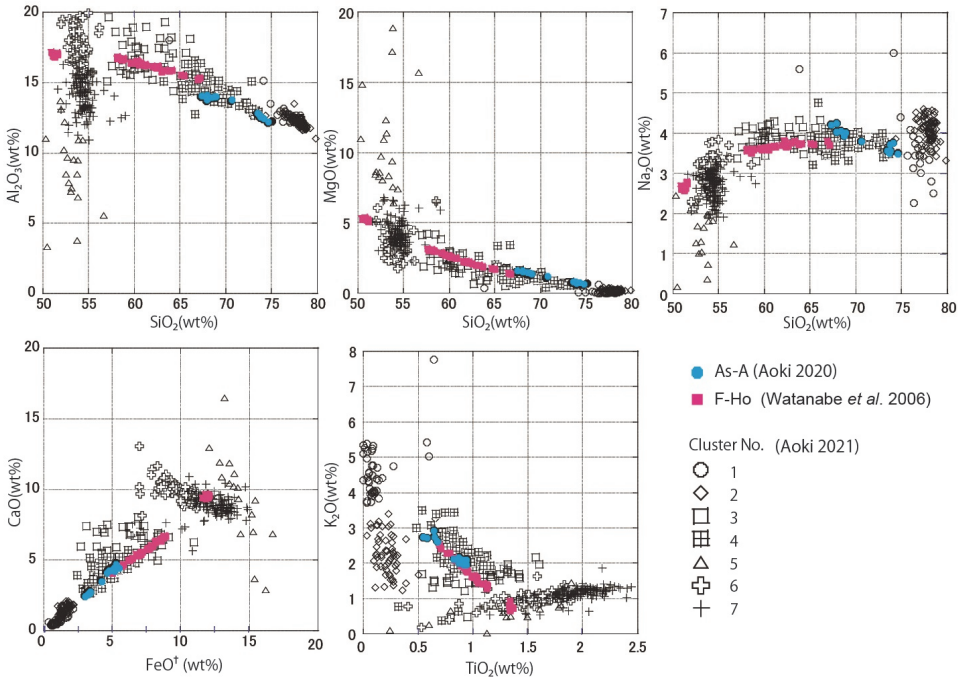


**Fig. 4** Plots of $SiO_2$-$Al_2O_3$, $SiO_2$-MgO, $SiO_2$-$Na_2O$, $FeO^{\dagger}$-CaO and $TiO_2$-$K_2O$ of volcanic glass shards. The geochemistry of volcanic glass shards is shown as follows: samples from the 0-9.50 cm interval in the MD01-2421 sediment core (Aoki 2021). The legend shows the clusters that were separated by cluster analysis using normalized data in Case A (Aoki 2021). As-A are shown in Aoki (2020). F-Ho are shown in Table 1 from Watanabe *et al*. (2006). †: Total iron is calculated as FeO.

Cluster No. 5, Cluster No. 6 and Cluster No. 7 in the MD01-2421 core are basaltic andesite groups (Fig. 2). The unit of Ho IV produced during the last stage of the 1707 AD eruption was characterized by basaltic magma (Fig. 3 and Table 1). The contents of $Na_2O$, $FeO^{\dagger}$, and MgO in the basaltic geochemistry of the F-Ho tephra do not overlap with Cluster No. 5. The $FeO^{\dagger}$ and

$TiO_2$ contents of Cluster No. 7 are greater than those of Cluster No. 6, and the $Al_2O_3$ content of Cluster No.7 is less than that of Cluster No. 6. This trend of geochemistry would suggest that the basaltic unit of F-Ho tephra resembled Cluster No. 6. The $SiO_2$ content in the basaltic geochemistry of the F-Ho tephra was 50-52 wt%, and it is slightly shifted from Cluster No. 6 in the MD01-2421 core. It might have been affected by microlites that might not have been sufficiently removed.

At this point, Cluster No. 6, Cluster No. 3, and a part of Cluster No. 4 of volcanic glass shards in the core top samples of MD01-2421 might be correlated to the F-Ho tephra. On the other hand, some volcanic glass shards of Cluster No. 4 in Fig. 4 shift away from a trend toward $FeO^{\dagger}$ and CaO content in F-Ho tephra and As-A tephra (Aoki 2021). It suggested that Cluster No. 4 contains volcanic glass shards from different source volcanoes or eruptive products in addition to F-Ho and As-A tephra. For future research, the Sakurajima Taisho eruption in 1914 AD (Sz-Ts tephra; Omori 1916) characterized by andesitic to dacitic magma should be analyzed and discussed as one of the correlative eruptions.

## 4. Summary

To search for cryptotephra at the top of core MD01-2421, Aoki (2021) reused the residues of foraminiferal research samples. As a result, there is a high possibility that samples in the top of core MD01-2421 might include the volcanic products of F-Ho tephra erupting from Mt. Fuji in 1707 AD in addition to As-A tephra erupted from Mt. Asama in 1783 AD.

Because geochemical variation of F-Ho tephra ranges from basaltic to dacitic, basaltic and andesitic clusters and a part of volcanic glass shards in a dacitic cluster among seven clusters of volcanic glass shards in the samples from core MD01-2421 might be correlated to the eruptive products of F-Ho tephra.

Some dacitic volcanic glass shards could not be correlated to either As-A tephra or F-Ho tephra; therefore, they should be reexamined to determine if they may correlate to another tephra, such as Sj-Ts tephra, which was characterized by andesitic to dacitic magma.

## Acknowledgments

The author has been using an EPMA since 2011 as one of the facilities in the Center for Advanced Marine Core Research of Kochi University (KCC), which is a nationwide joint-use system designed for scientists and students in Japan and is organized by the Ministry of Education, Culture, Sports, Science and Technology (MEXT). The data presented in this study are part of the tasks adopted in adoption numbers 16A029, 16B027, 17A053 and 17B053. I am especially grateful for support from Prof. Yuji Yamamoto (KCC) and Dr. Takuya Matsuzaki as technical staff (KCC) and administrative staff at Kochi University.

## References

Aoki, K. 2008. Revised age and distribution of ca. 87 ka Aso-4 tephra based on new evidence

from the northwest Pacific Ocean. *Quaternary International* **178**: 100–118.
Aoki, K., Irino, T. and Oba, T. 2008. Middle-late Pleistocene tephrostratigraphy of the sediment core MD01-2421 collected off the Kashima coast, Japan. *The Quaternary Research (Japan Association for Quaternary Research)* **47**: 391–407.**
Aoki, K. 2020. Major-element composition of volcanic glass shards in late Quaternary tephras provided from the Asama volcano in An-naka and Tomioka area, Gunma prefecture, central Japan. *Geographical Reports of Tokyo Metropolitan University* **55**: 1–11.
Aoki, K. 2021. The examination of cryptotephrostratigraphy performed by recycling the residue from samples used in a paleoceanographic study of foraminiferal fossils from the MD01-2421 sediment core collected off the Kashima coast of east Japan. *Geographical Reports of Tokyo Metropolitan University* **56**: 1–11.
Katoh, S., Danhara, T., Hart, W. K. and Gabriel, G. W. 1999. Use of sodium polytungstate solution in the purification of volcanic glass shards for bulk chemical analysis. *Nature and Human Activity* **4**: 45–54.
Koyama, M. 1998. Reevaluation of the eruptive history of Fuji volcano, Japan, mainly based on historical documents. *Bulletin of the Volcanological Society of Japan* **43**: 323–347. **
Le Bas, M. J. and Streckeisen, A. L. 1991. The IUGS systematics of igneous rocks. *Journal of the Geological Society, London* **148**: 825–833.
Miyaji, N. 1984. Wind effect on the dispersion of the Fuji 1707 tephra. *Bulletin of the Volcanological Society of Japan* **29**: 17–30. **
Oba, T., Irino, T., Yamamoto, M., Murayama, M., Takamura, A. and Aoki, K. 2006. Paleoceanographic change off central Japan since the last 144,000 years based on high-resolution oxygen and carbon isotope records. *Global and Planetary Change* **53**: 5–20.
Omori, F. 1916. Chapter V. Accumulation and transportation of ashes thrown out during the Sakura-jima eruptions of 1914 (the Sakura-jima eruptions and earthquakes ii [On the sound and ash-precipitation areas of, and on the level changes caused by, the eruptions of 1914, with historical sketches of earlier Sakura-jima outbursts]). *Bulletin of the Imperial Earthquake Investigation Committee* **8**: 113–133.
Tsuya, H. 1955. Geological and petrological studies of Volcano Fuji V: on the 1707 eruption of Volcano Fuji. *Bulletin of the Earthquake Research Institute* **33**: 341–383.
Watanabe, S., Widom, E., Ui, T., Miyaji, N. and Roberts, A. M. 2006. The evolution of a chemically zoned magma chamber: The 1707 eruption of Fuji volcano, Japan. *Journal of Volcanology and Geothermal Research* **152**: 1–19.

(*: in Japanese, **: in Japanese with English abstract)